

1 **Mud volcanoes influences on the seismicity behaviors indicated from z and b value**

2 **Gege Hui^{1,2*}, Gangzhi Li^{1,2}, Chuang Sun^{1,2}, Yipeng Zhang^{1,2}, Pengcheng Wang³, Peizhen Zhang^{1,2}**

3 ¹ Guangdong Provincial Key Laboratory of Geodynamics and Geohazards, School of Earth Sciences and
4 Engineering, Sun Yat-Sen University, Guangzhou, 510275, China

5 ² Southern Marine Science and Engineering Guangdong Laboratory (Zhuhai), zhuhai, 519082, China

6 ³ Ocean University of China, Qingdao 266100, China

7 Corresponding author: Gege Hui (huigg@mail.sysu.edu.cn)

8 † Present address: *School of Earth Sciences and Engineering, Sun Yat-sen University (SYSU), Zhuhai Campus,*
9 *Tangqi Road, Tangjiawan, Xiangzhou District, Zhuhai, Guangdong, 519082, P.R.China.*

10 **Key Points:**

- 11 • b-values in the SW Taiwan show the frequently periodicity fluctuations.
- 12 • z-values in the mud volcanoes area keep seismic quiescence before a big shock.
- 13 • A conjunct triggering relationships should exist between mud volcanoes and earthquakes.

14

15 **Abstract**

16 To explore the repeating mud volcanoes influences on the seismicity behaviors, we measured the
17 spatial distribution z and b value changes with the time in the mud volcanoes developing area.
18 We find a weak correlation between the b - z values and the mud volcanoes. Generally, the z -
19 values anomalies of the mud volcanoes area show unchanged negative values and indicate the
20 seismic quiescence before a strong earthquake, while the b -values show the frequently
21 periodicity fluctuations around the value of 0.5. It may indicate the conjunct triggering
22 relationships between the mud volcanoes and earthquakes stuck. We inferred that the mud
23 volcanoes eruptions help to partition and release part of the regional stress accumulation from the
24 earthquake seismogenic structures, thus balanced the local stress in the strata.

25 Keywords: Mud volcano; SW Taiwan; coulomb stress change; b - z -value; conjunct triggering
26 relationship

27 **Plain Language Summary**

28 Earthquakes caused subsurface fracture and stress perturbation are known to induce the
29 earthquakes. While, the spatial and temporal distribution features of the seismicity activity before
30 and after the mud volcanoes eruptions remain uncertain. This study analyzes the relationship
31 between the strong earthquakes sequence including the SW Taiwan offshore December 26th,
32 2006 and June 5th, 2016 earthquakes and the z and b values anomalies in the mud volcanoes
33 developing area. Our results reveal the z -value in the offshore SW Taiwan shows the seismic
34 quiescence before a big shock, but without many strong earthquake's occurrence. It may suggest
35 a conjunct triggering relationships between the mud volcanoes and earthquakes stuck, the mud
36 volcanoes eruptions would be an effective way to partition and release part of the regional stress
37 accumulation from the earthquake seismogenic structures, thus balanced the local stress in the
38 strata to mitigate large magnitude seismicity.

39 **1 Introduction**

40 Mud volcanoes are of particular interest for several reasons. The scientists have investigated it
41 for a couple of decades, because it closely related to the gas hydrate accumulations and is
42 important for the global carbon cycle, which have been used successfully to predicting the
43 offshore oil and gas assembly (Etiope et al., 2004; Davies and Stewart, 2005; Kopf and
44 Deyhle, 2006). Mud volcanoes can occur in different geological settings, especially the fore-arc
45 basins on active continental margin, or in the petroliferous basins on the passive continental
46 shelves (Planke et al., 2003). It presented and recognized as the specific phenomenon similarly to
47 the magma volcanisms. Always, the mud volcano shows chaotic acoustically amorphous
48 piercement structures (Dia et al., 1999; Martinelli and Panahi, 2005) and the anticlines or the trust
49 faults, to be the feeder channel, for the semi-liquid argillaceous material migrating directly along
50 the narrow faults or fissures in the upper layer (Yusifov, 2005).

51 Mud volcanism has a long history of investigation. A number of research papers have
52 consolidated the strain and stress perturbations from large earthquakes would affect the mud
53 volcanoes and ground water at a long distance (Delisle et al., 2002) and such instances are widely
54 reported, such as the Pakistan, Romania, Sumatra and etc. Snead et al. (1964) has done the
55 quantitatively study and examined effects of different magnitude thresholds and triggering
56 distances on mud volcanoes. Following, many studies (Milkov et al., 2003; Mellors et al., 2007;

57 [Maestrelli et al.,2013](#)) have consolidated the hypotheses that whether the mud volcanoes are
58 developed as the earthquake environmental effects. The recent example of the earthquake/mud
59 volcano triggering occurred on the Arabian Sea, the new islands have been created during the
60 process. Sedimentary analysis shows two islands are composed of pale bluish grey clay as well
61 as grey mudstone blocks uplifted rapidly when the Mw7.7 earthquake occurred 180 miles away
62 from coastlines of the Arabian Sea in 1945 ([Dimitrov,2002](#)). The similar situation occurred 16
63 km offshore in Gwadar west bay, and the islands with circular coned-shape encrusted with
64 marine sediments, the gas eruptions and flames were also noticed in the vicinity of the new
65 island ([Sondhi,1947](#)). All these new created islands were found kilometers away from the
66 epicenter after the earthquake and only the coseismic uplift can rule out ([Mellors et al.,2007](#);
67 [Rudolph and Manga,2010;2012](#); [Bonini Hui et al., 2018](#);[Hui et al., 2018](#)).

68 The mud volcanoes in offshore SW Taiwan mainly distributed on the Kaoping slope ([Figure1a](#);
69 [Chen et al.,2014](#); [Chiang et al., 2020](#)). Many submarine volcanoes, diapirs and deep-incised
70 canyons have been recognized and mostly developed along the axis of the fold anticlines or the
71 thrust faults deformation front. What's more, there are numerous earthquakes larger than Mw5.0
72 have been reported in the SW offshore Taiwan slope ([Chen et al.,2014](#)). [Hui et al.\(2018\)](#) have
73 confirmed that the majority of mud volcanoes occurred immediately after the strong mainshock
74 and confirmed to be perturbed by the stress change produced in the ground shaking.

75 Whereas, the mud volcano is symbolized with gashydrate and oil accumulation, it has multi-
76 stage eruptions on the seismic profile indication and can be re-activated when the next
77 earthquake struck ([Kumar et al.,2018](#)). This process will rework or destroy the accumulation
78 environment on the slope, even to trigger the seabed instability and change the local stress field.
79 Thus, the further research is needed, such as to confirm how the mud volcanoes influences on the
80 seismicity behaviors mud volcano eruption environment influences on the earthquakes behaviors
81 in the multi-phase MV eruption zone.

82 Generally, the high b-value can indicate the small-scale earthquake event when the parameter a
83 keeping constant ([Wimer,2001](#); [Leptokaropoulos and Lasocki,2020](#)). In contrast, the low b-value
84 indicating the relative high stress status in the crust would hold another earthquake event.
85 Another seismicity parameter z describes the seismic rate ([Scholz,1968](#)). z-value varies in the
86 specific regions, and show different seismic rates in different period before the mainshock. For
87 decades, the seismic rate (z-value) has been used to obtain the precursory information of
88 earthquakes. For example, [Wiemer and Wyss \(1994\)](#) has identified the seismic quiescence before
89 the Landers (M=7.5) and Big Bear (M=6.5) 1992 earthquakes. Historical statistical results have
90 demonstrated the law that the b-value decreases to negative when a mainshock approaching, and
91 the seismic risk probability increases as the b-z-value becomes positive. Determining the crustal
92 b-z values under which earthquake can occur is of tremendous importance to seismicity
93 evaluation in our study area. Based on the regional geological condition, we applied the b-z
94 value spatial scanning image and the abnormal area to conclude the precursory period prior to
95 the occurrence of large crustal earthquake. Finally, we can ensure the multiphase mud volcanoes
96 influence on the seismicity activity.

97 In this study, we took advantage of the Taiwan Telemetered Seismic Network (TTSN) and
98 Global Centroid-Moment-Tensor (CMT) Project for compiling the seismic earthquake catalogue,
99 and the important b- z-value in the precursory of the earthquake, which have been used to study
100 the triggering relationship between the mud volcanoes and earthquakes offshore SW Taiwan. It
101 would help us a better understanding of the resource and geohazard effect of MV, and provide
102 new perspectives for the disaster prevention and mitigation, as well as the resources evaluation.

103 2 Data description

104 2.1 Earthquake and mud volcano catalogue

105 The earthquake catalogue in this study compromise tens thousands of historical seismicity
106 activities,our study area is located in SW offshore Taiwan where seismic activity is the weakest
107 and with the scarcely large magnitude earthquakes occurrence (Figure1a). While remarkably, 10
108 NE-NNE-striking elongated mud diapir belts have developed in the deeper water of the Kaoping
109 Slope on SW Taiwan continental slope(Liu et al., 2000; Chen et al.,2003; Sung et al.,2010).
110 Moreover, 60 mud volcanoes are recognized in the study area surrounded by the thrust faults,
111 and the gas fluids migrated upward along the fractures (Yin,1986; Chen et al.,2003; Chiu et
112 al.,2006). The majority of the mud volcanoes extend southward, mainly distributed along the
113 NNE–SSW to N–S direction against with the canyon system (Chow et al.,2001; Lacombe et
114 al.,2004; Hai et al.,2007). Previous study from the seismic reflections show the diapirs are almost
115 exposed at the seafloor and covered only by thin sediments, indicating they are still active and
116 growing (Chen et al.,2014; Hui et al.,2018). Submarine mud volcanoes are different from the
117 onshore, which are much younger than onshore, and most active (You et al.,2004). Many of them
118 are found at the water depths larger than 1000km.

119 The mud volcanoes catalog in this study is a compendium of events over 70 times in the former
120 studies and includes historical as well as instrumentally recorded events, which showed the
121 occurrence short time after moderate to large offshore earthquakes ($M > 5.0$) (Wang et al.,1988;
122 Kao and Chen,2001; Rau et al.,2000; Chuang et al.,2013). We have compiled the catalog ranging
123 from the 2003 to 2016. According to the statistical results in FigureS1, it shows several moderate
124 to strong earthquakes occurrences roughly been divided into three active seismic periods. In
125 sequence, the first period M_w 5.2 26 December 2006 earthquake initiated in the SW offshore
126 Taiwan was followed with 12 hours later by two strong mainshocks at 27 December 2006, the
127 largest of which had the magnitude of M_w 6.7. The second seismic period started from 04 March
128 2010, and the seismic intensities gradually decreased with the M_w 5.4 earthquakes at 24
129 February 2012. The latest period strong earthquake is occurred at 05 February 2016 with the
130 magnitude of M_w 6.11. All these events in the SW offshore stuck an approximately 10-30 km
131 distance extending from the Taiwan Island, which have impressive coseismic effect in the
132 epicenter and its vicinity area(FigureS2).

133 2.2 Correlation between the seismic sequence and mud volcano eruptions in SW offshore 134 Taiwan

135 For an alternate estimate of the earthquake mud volcanoes, we use the eruption time-of-
136 occurrence information (FigureS1). According to the graph in FigureS1, which has incorporated
137 the Number-Time (N-T) histograms from the earthquakes and mud volcanoes, it can be seen that
138 the earthquakes number sharply went up to the summit at each time the strong mainshock stuck.
139 We can clearly see that the N-T fluctuation curves with the impulse-shake patterns with each
140 strong earthquake, while the mud volcanoes show the platform signals with a long duration
141 explosion. In the 12 years spanning from 2005 through 2016, the N-T chart shows a positive
142 correlation between the mud volcano and the earthquakes occurrences. As is demonstrated in the
143 red histograms, we can see a considerable number of mud volcano eruptions increases since from
144 26 December 2006, with the similar trend of the earthquake number and moment magnitude.
145 Except this, there are the same situations occurred at the year of 2010 and 2016, when there are
146 two strong earthquakes stuck. The overall process like years between eruptions show the

147 exponential Poisson expected shape. Besides, what calls for special attention is that there has a
 148 small transient gap and eruption time delay between the earthquakes and the mud volcanoes.
 149 Generally, the eruption of MV occurred one or two days subsequential to one mainshock and can
 150 even last for several years, or the reposed MV even been re-activated.

151 **3 Materials and Methods**

152 3.1 Analysis on the seismic data catalogue

153 The seismic observation technology development in the vicinity of Taiwan has multi-phase, and
 154 was initiated from the year of 1897. The third period development was happened during the 1973
 155 to 1990, and the TTSN was set up. The recent network can document the earthquakes magnitude
 156 smaller than 1.0, and acquire more accurately recording of the earthquakes in Taiwan. In this
 157 study, we have compiled the earthquake catalog from 1980 with at least 15000 events. According
 158 to the focal mechanisms difference, the seismic activities have been divided into four seismic
 159 zones (A,B,C,D in Figure1a, Wang and Shin, 1998). The SW seismic zone activity is most weak
 160 in the Taiwan area and the earthquakes show the shallow centroid focal depth less than 20km.

161 From the Magnitude-Time (M-T) diagram (FigureS3), we can see three to four seismic
 162 reoccurrences, there are the years of 2000, 2000-2010 and 2015, respectively and the average
 163 reoccurrence interval is about five years. In addition, the four M-T histograms show the average
 164 seismicity activity of the moderate-strong earthquake in different area, the observed earthquakes
 165 number increased with the time when the magnitude is larger than 5.5.

166 To estimate the earthquakes catalog completeness and discuss the data dependence on the
 167 seismic network, we calculated the Minimum Magnitude of Completeness (M_c) which reflected
 168 the advancement of the seismic monitoring and analysis methods (Figure1b). This calculation is
 169 relying on the integrated study on frequency-magnitude distribution (FMD) of the seismic
 170 activities. The FMD is calculated as follow function:

$$R(a, b, M_i) = 100 - \left(\frac{\sum_{M_i}^{M_{max}} |B_i - S_i|}{\sum_i B_i} 100 \right)$$

171 B_i is standing for the accumulation number for every strong earthquake; S_i stands for the assumed
 172 accumulation number, this process is to confirmed the fitting degree between them. We
 173 evaluated the M_c value of the earthquakes ranging from 1995 to 2020 by the open source
 174 software ZMAP5.5 software in MATLAB (Wimer,2001; Leptokaropoulos and Lasocki,2020).
 175 The result shows that the M_c has fluctuations within a narrow range since the year of 2000, and
 176 show an overall descending trend. The Goodness of FMD fit to power law displays the M_c at
 177 90% confidence to 3.9 (Figure1c). Based the M_c value above, we select the reasonable and
 178 homogeneous seismicity, removed the inadequate and explosions from earthquake catalog for
 179 calculation.
 180

181 3.2 z-value statistical method

182 Generally, the z-value is widely used to testify and quantitatively calculating on the seismic rate
 183 of the seismic activity, two aggregate functions $AS(t)$ and $LTA(t)$ have been employed in the
 184 calculation (Wimer,2001). z-value is aim to evaluate and make comparisons of the seismic rate
 185 in different time intervals approaching to a main shock. In other words, if we set four different
 186 times with equal intervals before one earthquake event, and the z-value will be defined to be
 187 positive when the accumulative seismic occurrence between t_1 and t_2 is larger than that between

188 t_3 and t_4 . In this case, the positive z-value can indicate the decreasing seismic rate. $AS(t)$ Function
 189 is often simplified as:

$$Z(t) = \frac{(R_1 - R_2)}{\sqrt{\frac{\sigma_1^2}{n_1} + \frac{\sigma_2^2}{n_2}}}$$

190 where the R_1, R_2 represent the average seismic activity rate obtained by using a certain time
 191 interval as the sampling interval in period 1 (from t_0 to t_e) and period 2 (from t to t_e),
 192 respectively; σ_1 and σ_2 are the standard deviation of seismic activity rate in the corresponding
 193 period; n_1 and n_2 are the number of samples in the corresponding period. $AS(t)$ Function is used to
 194 resolve on a very crucial question: when is the maximum single seismic rate change occurred
 195 between two specific ends on the timeline? It is useful to identify one anomaly at the end of a
 196 time series, but it cannot detect two or more seismic rate change anomalies in the time series.
 197 Thus the $LTA(t)$ function is introduced, it is more effective for the unbiased statistical test and the
 198 detection of multiple anomalies in a time series. The formula for the $LTA(t)$ function is defined as
 199 follows:
 200

$$Z(t) = \frac{(R_{all} - R_{W_t})}{\sqrt{\frac{\sigma_{all}^2}{n_{all}} + \frac{\sigma_{W_t}^2}{n_{W_t}}}}$$

201 where the R_{all}, R_{W_t} represent the overall average seismic activity rate and the average seismic
 202 activity rate within the time window with a length of W_t . Moreover, the seismic catalogue
 203 aftershocks clusters elimination and integrity analysis should be completed before using the
 204 above function to calculate the z value.
 205

206 We used the earthquakes background through the entire Taiwan Island and its vicinity area. The
 207 calculation used the minimum latitude as 20° and the maximum latitude as 26° , the longitude
 208 ranges from the 118° to 124° . The spatial scanning distance increment of longitude and latitude is
 209 0.02 degrees. The starting time T_0 is set as 1985, and the end time T_e is the year of 2005. The
 210 starting time window T_c is 1997, and the average window length Tw is 5 years. In the
 211 calculation, the earthquakes magnitude constraint is the M_c greater than or equal to 2.0, and the
 212 focal depth is less than or equal to 50 km. In addition, we adopted the sampling parameters such
 213 as the time step to be 30 days. And as a rule of thumb, we successfully use $n_i = 20$ as the
 214 calculation lattice. Then we select the LTA function under "time-cut" mode and plot the
 215 latitude/longitude map of z-values at a specific time T (Figure 5 a-n). We take the time of half a
 216 year before and after each main shock as the statistical time window, the number of earthquakes
 217 within a radius of 10 km is captured spatially with each main shock epicenter. Generally, the
 218 negative z-value within 10 days before an earthquake can indicate the probability of the
 219 earthquake risk is becoming higher (Wyss and Martyrosian, 1998). Therefore, we can confirm the
 220 statistical effects of earthquakes with different spatial scales, from observing the near field z-
 221 value changes before the occurrence of large earthquakes.

222 3.3 b-value statistical method

223 b-value plays an important role in Gutenberg-Richter (GR) earthquake frequency-magnitude
 224 relationship. Similar to the z-value discussed above, estimation of the b value is crucial for

225 evaluation of the earthquake occurrence probability. The G-R relationship put forward by
 226 [Gutenberg and Richter \(1944\)](#) can be described as follows:

$$\log N = a - bM$$

227
 228 where b in the function stands for the slope and are measured as a function of depth in a wide
 229 variety of tectonic regions; N is the accumulative number of seismic activities having magnitude
 230 larger or equal to M ; M is the magnitude of the event. The cumulative frequency - magnitude has
 231 a linear distribution.

232 Changes of b -values as a function of time would provide a signal for evaluating the regional
 233 crustal stress accumulation status before or after the mainshock ([Scholz,1968](#); [Shi and Bolt,1982](#);
 234 [Rao et al.,2005](#)). When the number of large earthquakes is large, the b value will be relatively
 235 small, so the area with small b value is often considered to have a relatively large chance to
 236 occur on a large magnitude ([Smith,1981](#)).

237 In the previous study, there several methods like WLS (weighted least squares method) and max
 238 L (maximum likelihood) are offered for the calculation on the changes of b -values, but both
 239 methods of estimating b -values show the similar results.

240 z -maps from a to n shown in the [Figure2](#) have been calculated with the time increment of 5
 241 years, and the z -values were plotted in each slide with different colors representation for
 242 assessing the outstanding anomalies. In addition, the b value changes with the time ([Figure3a](#))
 243 and map of the maximum z values of all LTA functions with a window length of 3 yr have been
 244 plotted ([Figure3b](#)). Particularly, several significant strong earthquakes have also been taken
 245 account into the calculation. The objective of the study is to determine whether there was the
 246 significant rate decrease prior to the big shock in this area, and what might occur at the mud
 247 volcanoes developing area.

248 **4 Results**

249 As mentioned in the last paragraph in the last section, b - z -value changes are the significant
 250 earthquake precursor signals, which can possibly provide the valid information like the location,
 251 time and magnitude for a big shock. Many previous studies have worked on the b - z -value
 252 changes before the mainshock. [Wu et al. \(2006,2008\)](#) have conducted the b - z -value changes
 253 research and the distribution maps were drawn for the half year, one year and two years
 254 separately before the big earthquakes. According to the statistical data, when approaching to a
 255 big earthquake, the b value at the epicenter decreases gradually and even presents negative.
 256 Different b value changes with time before the earthquake have different indications. According
 257 to the historical observation, b value in the epicenter present the negative accounted for only
 258 47.0% two years before earthquake (16negative, 18positive, three zero, three has no obvious
 259 data). While to half a year before the earthquake, negative b value of the epicenter rate up to
 260 71.4% (25 negative, 10positive, five zero), and b values in most of the earthquake epicenter
 261 show the decreasing phenomenon ([Wang et al.,2004](#)). What's more, they indicated that the z -
 262 value have the similar trend to the b -value, it would decrease as well when approaching a big
 263 earthquake ([Wyss and Martyrosian,1998](#); [Wyss et al.,1996](#)).

264 4.1 spatially distribution of the z -value

265 The first prominent variations in the seismicity pattern can be identified in 1990 ([Figure2d](#)), it
 266 can easily identify the high z values in [Figure2c](#) decreased and even transited from positive to
 267 negative (declined to -2.0) in an area 15 km north of the epicenter, along the rupture of the 1990
 268 M_w 6.7earthquake. Similarly, it has been noticed in this map ([Figure2d](#)), the z -value have a

269 drastically decline two or three months before another two earthquakes with magnitudes of 6.0
270 and 6.1. Except this, the z-values have the similar trend have been detected, for instance, the M_w
271 6.8 earthquakes in 1995 (Figure2e), the M_w 6.4 earthquake in 2000 (Figure2f), the M_w 7.06
272 earthquake in 2005 (Figure2g) and so on. The z-map coloring pattern show an overall decreasing
273 with the time approaching to the strong earthquakes, and the z-value of the epicenter changes
274 even gradually changes from positive to negative (on the map, it changes from red to blue).
275 Particularly, on the z-value map of the 2019 Hualian earthquake (Figure2n) and another
276 December 26th,2006 (Figure2h) event, z-value displays with the sharp decline and it even shows
277 negative values spreading the whole study area hours before a big earthquake.
278 Obviously, all the z-value results indicate that there was the significant rate decrease prior to the
279 big shock in the study area consolidated the previous study. However, there are exceptions that
280 the z-values in the offshore SW Taiwan keep negative since from 1980 until now and seems to
281 retain the seismic quiescence before a big earthquake. But only two historical strong earthquakes
282 (with magnitude larger than 6.0) have been recorded in this mud volcanoes developing area. It
283 seems violate the observation and is inconsistent with theories that the negative z-value are
284 almost always occurred before a strong earthquake.

285 4.2 b-z value changes with time

286 To the further study of the b-z-values distribution in the mud volcanoes area, we have also
287 calculated the temporal variation in b-value (Figure3a) and the maximum z values (Figure3b) in
288 the LTA function. The cumulative number change with time is shown (blue line in Figure3). We
289 selected the earthquake catalogue with the longitude ranges from 120° to 121° and the latitude
290 from 21.5° to 23°. According to the b-values in Fig. 3a, it can be recognized that in the one-year
291 period before the December 26th,2006 M_w 6.75 earthquake in our mud volcanoes developing
292 area, the b-values are higher than in most other periods, and show a brief decline after the
293 earthquake. Compared with the 2006 M_w 6.75 earthquake, the b-values before and after the
294 2010, 2012 and 2016 big earthquakes have shown the same b changes in time (green stars in
295 figure 3a). Based on the previous study, the b value of the epicenter should decrease even to
296 negative at the interval of two years till to half a year before the earthquake. But the overall
297 earthquakes characteristics in SW Taiwan mud volcanoes area show the positive low b-values
298 and frequently fluctuations.

299 5 Discussion and Conclusion

300 Traditionally, there are many controlling factors on the b-value change. One is the stress
301 redistribution accommodate by the faulting activity, which is characterized by the earthquakes or
302 the other eruptions (Hsu et al.,2008; Lacombe et al.,2001). Another one is because of the
303 underground random fissures or ruptures, large rupture would result in decrease of b-value, while
304 small fissures would increase the b-value (Ghosh et al.,2008; Scholz,2019). Through the analysis
305 on the b-z-values of the mud volcanoes area in SW Taiwan, we can find that the b-values of
306 earthquakes between 1995 and 2020 show the frequently periodic fluctuations and lacking of the
307 big earthquakes, only with five to six moderate-strong earthquakes. Especially, only the
308 December 26th,2006 M_w 6.75, M_w 6.54 earthquakes occurred offshore and the February
309 5th,2016 M_w 6.11 earthquake occurred onshore in SW Taiwan (A and B in the Figure 3b).
310 According to the b-value distribution, it has the average value around 0.5 and fluctuations with
311 small amplitude, it may demonstrate the relatively high seismic rate in this study area due to the
312 slowly stress redistribution and accommodation by small fissures.

313 In a more complex scenario, the regional subduction- accretionary geological settings in this
314 study area are particularly susceptible to the neotectonic activity, it is likely triggering numerous
315 small-scale fissures and the small earthquakes. These small earthquakes ruptures can be acted as
316 the feeder dikes for the deep argillaceous rocks ascending to the upper layer, thus causing the
317 mud volcanoes eruptions (Chen et al.,2003; Wu et al.,2005; Yin et al.,2015). In addition, the
318 Taixinan Basin have received with great thickness of marine facies sediments since the Pliocene,
319 which can provide with the favorable overpressure uncompact onshore shale formation and
320 offshore marine facies mudstone formation deposits. The crustal stress might potentially disturb
321 by the earthquakes induced local ground water equilibration, regional stress filed redistribution
322 and accommodation (by mud volcanoes eruptions), thus showing the relative high b-value (that
323 is, the stress would slowly release by the small fissures when the local stress accumulative to a
324 considerable amount and show the negative z-value).

325 On the basis of observations of the b-value, we can conclude the mud volcanoes eruptions and
326 earthquakes promote and restrain each other and induce the periodic crustal stress accumulation
327 and release. This influenced the b-z-values distribution indicated the conjunct triggering
328 relationships between mud volcanoes and earthquakes. Among them, the mud volcano eruptions
329 can help to allocate and release part of the regional stress accumulation in the study area from the
330 earthquake seismogenic structures, thus prevented the stress accumulation for a strong
331 earthquake. Therefore, it can well demonstrate why the z-value in the offshore SW Taiwan
332 always show the seismic quiescence before a big shock, but without many strong earthquakes
333 occurred. Moreover, the conjunct triggering relationships between the mud volcanoes and the
334 earthquakes give good explanations on the b-value in the mud volcanoes area keeping steady and
335 showing periodicity fluctuations.

336 **Acknowledgments, Samples, and Data**

337 This research was jointly supported by the National Postdoctoral Program for Innovative Talents
338 (BX20190391),Guangdong Province Introduced Innovative R&D Team of Geological Processes
339 and Natural Disasters around the South China Sea (2016ZT06N331), the Guangdong Basic and
340 Applied Basic Research Foundation (No.2019A1515110305). The Project financially funded by
341 the Fundamental Research Funds for the Central Universities (No.201gpy37), and the National
342 key Research and Development Program of China (2017YFC1500102).We also thank the
343 operators of the Broadband Array in Taiwan for Seismology (BATS) for making available their
344 earthquake catalog.

345 All the dataset enclosed in this paper are available and can be cited from “hui, gege (2020),
346 “Gege Hui et al.,2020.Triggering relationship between the mud volcanoes and earthquakes
347 offshore SW Taiwan,Journal of Geophysical Research: Solid Earth”, Mendeley Data, V2, doi:
348 10.17632/n67dy87vdg.2 <http://dx.doi.org/10.17632/n67dy87vdg.2>”.

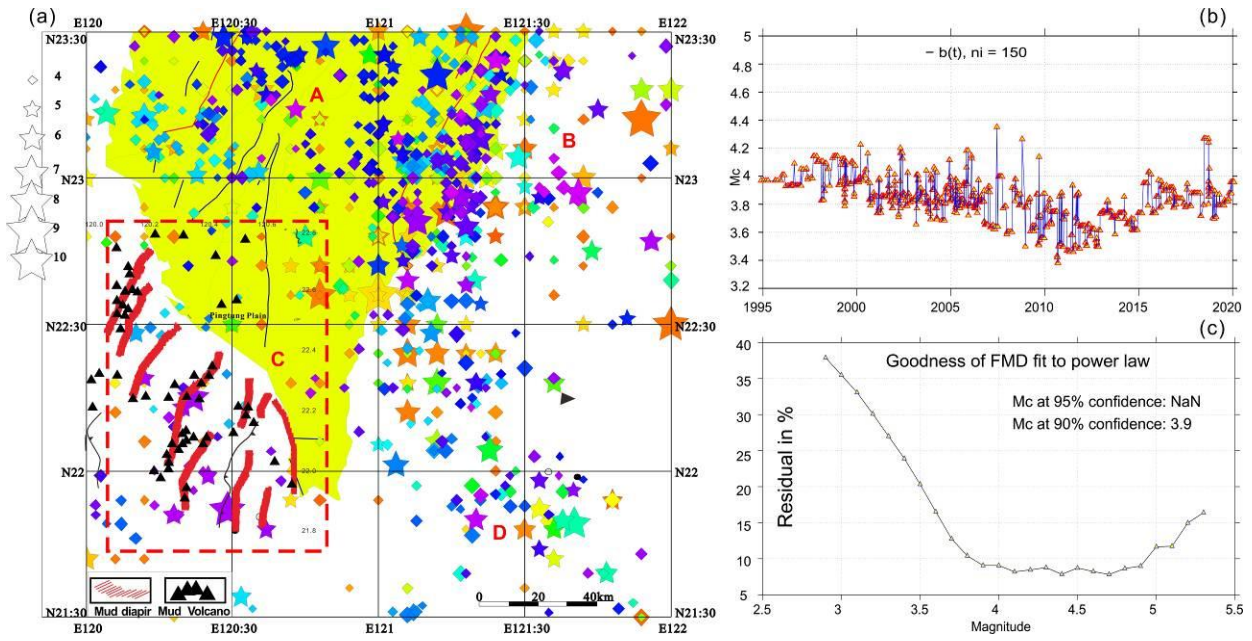
349 **References**

- 350 Bonini, M., Maestrelli, D., & Manga, M. (2018). Structural setting and earthquake triggering of
351 mud volcanoes: examples from Azerbaijan and Italy. EGUGA, 19176.
352 Chen, S. C., Hsu, S. K., Wang, Y., Chung, S. H., Chen, P. C., Tsai, C. H., ... & Lee, Y. W.
353 (2014). Distribution and characters of the mud diapirs and mud volcanoes off southwest
354 Taiwan. *Journal of Asian Earth Sciences*, 92, 201-214.

- 355 Chen, Y. C., Sung, Q., & Cheng, K. Y. (2003). Along-strike variations of morphotectonic
356 features in the Western Foothills of Taiwan: tectonic implications based on stream-gradient
357 and hypsometric analysis. *Geomorphology*, 56(1-2), 109-137.
- 358 Chiang, C. S., Hsiung, K. H., Yu, H. S., & Chen, S. C. (2020). Three types of modern submarine
359 canyons on the tectonically active continental margin offshore southwestern
360 Taiwan. *Marine Geophysical Research*, 41(1), 1-17.
- 361 Chiu, J. K., Wei-Hao, T., & Liu, C. S. (2006). Distribution of gassy sediments and mud
362 volcanoes offshore southwestern Taiwan. *TAO: Terrestrial, Atmospheric and Oceanic
363 Sciences*, 17(4), 703.
- 364 Chow, J., Lee, J. S., Liu, C. S., Lee, B. D., & Watkins, J. S. (2001). A submarine canyon as the
365 cause of a mud volcano—Liuchieuyu Island in Taiwan. *Marine Geology*, 176(1-4), 55-63.
- 366 Chuang, R. Y., Johnson, K. M., Wu, Y. M., Ching, K. E., & Kuo, L. C. (2013). A midcrustal
367 ramp - fault structure beneath the Taiwan tectonic wedge illuminated by the 2013 Nantou
368 earthquake series. *Geophysical Research Letters*, 40(19), 5080-5084.
- 369 Davies, R. J., & Stewart, S. A. (2005). Emplacement of giant mud volcanoes in the South
370 Caspian Basin: 3D seismic reflection imaging of their root zones. *Journal of the Geological
371 Society*, 162(1), 1-4.
- 372 Deli, D. (1991). Characteristics of geologic structure and hydrocarbon potential of the southwest
373 Taiwan basin. *Marine Geology & Quaternary Geology*, (3), 3.
- 374 Delisle, G., Von Rad, U., Andruleit, H., Von Daniels, C., Tabrez, A., & Inam, A. (2002). Active
375 mud volcanoes on-and offshore eastern Makran, Pakistan. *International Journal of Earth
376 Sciences*, 91(1), 93-110.
- 377 Dia, A. N., Castrec-Rouelle, M., Boulegue, J., & Comeau, P. (1999). Trinidad mud volcanoes:
378 where do the expelled fluids come from?. *Geochimica et Cosmochimica Acta*, 63(7-8),
379 1023-1038.
- 380 Dimitrov, L. I. (2002). Mud volcanoes—the most important pathway for degassing deeply buried
381 sediments. *Earth-Science Reviews*, 59(1-4), 49-76.
- 382 Etiope, G., Feyzullayev, A., Baciu, C. L., & Milkov, A. V. (2004). Methane emission from mud
383 volcanoes in eastern Azerbaijan. *Geology*, 32(6), 465-468.
- 384 Ghosh, A., Newman, A. V., Thomas, A. M., & Farmer, G. T. (2008). Interface locking along the
385 subduction megathrust from b - value mapping near Nicoya Peninsula, Costa
386 Rica. *Geophysical Research Letters*, 35(1).
- 387 Gutenberg, B., & Richter, C. F. (1944). Frequency of earthquakes in California. *Bulletin of the
388 Seismological Society of America*, 34(4), 185-188.
- 389 Hai, Y., Guangjian, Z., & Jinfeng, M. (2007). Fracture characteristics and basin evolution of the
390 Taixinan basin in Cenozoic. *Petroleum Geology and Experiment*, 29(6), 560.
- 391 Hsu, S. K., Kuo, J., Chung-Liang, L., Ching-Hui, T., Doo, W. B., Ku, C. Y., & Sibuet, J. C.
392 (2008). Turbidity currents, submarine landslides and the 2006 Pingtung earthquake off SW
393 Taiwan. *TAO: Terrestrial, Atmospheric and Oceanic Sciences*, 19(6), 7.
- 394 Hui, G., Li, S., Wang, P., Zhu, J., Guo, L., Wang, Q., & Somerville, I. D. (2018). Neotectonic
395 implications and regional stress field constraints on mud volcanoes in offshore southwestern
396 Taiwan. *Marine Geology*, 403, 109-122.
- 397 Kao, H., & Jian, P. R. (2001). Seismogenic patterns in the Taiwan region: insights from source
398 parameter inversion of BATS data. *Tectonophysics*, 333(1-2), 179-198.

- 399 Kopf, A., & Deyhle, A. (2002). Back to the roots: boron geochemistry of mud volcanoes and its
400 implications for mobilization depth and global B cycling. *Chemical Geology*, 192(3-4),
401 195-210.
- 402 Kumar, A., Yang, T. H., Walia, V., Sung, Y. C., Lee, H. F., Lin, S. J., & Wen, K. L. (2018).
403 Characterization of some selected mud volcanoes of southern Taiwan. *Acta*
404 *Geophysica*, 66(5), 1257-1265.
- 405 Lacombe, O., Angelier, J., Mouthereau, F., Chu, H. T., Deffontaines, B., Lee, J. C., ... & Siame,
406 L. (2004). The Liuchiu Hsu island offshore SW Taiwan: tectonic versus diapiric anticline
407 development and comparisons with onshore structures. *Comptes Rendus*
408 *Geoscience*, 336(9), 815-825.
- 409 Lacombe, O., Mouthereau, F., Angelier, J., & Deffontaines, B. (2001). Structural, geodetic and
410 seismological evidence for tectonic escape in SW Taiwan. *Tectonophysics*, 333(1-2), 323-
411 345.
- 412 Leptokaropoulos, K., & Lasocki, S. (2020). SHAPE: A MATLAB Software Package for Time -
413 Dependent Seismic Hazard Analysis. *Seismological Research Letters*, 91(3), 1867-1877.
- 414 Liu, J. Y., Chen, Y. I., Pulinets, S. A., Tsai, Y. B., & Chuo, Y. J. (2000). Seismo - ionospheric
415 signatures prior to $M \geq 6.0$ Taiwan earthquakes. *Geophysical research letters*, 27(19), 3113-
416 3116.
- 417 Martinelli, G., & Panahi, B. (Eds.). (2005). *Mud Volcanoes, Geodynamics and Seismicity:*
418 *Proceedings of the NATO Advanced Research Workshop on Mud Volcanism,*
419 *Geodynamics and Seismicity, Baku, Azerbaijan, from 20 to 22 May 2003 (Vol. 51).*
420 Springer Science & Business Media.
- 421 Mellors, R., Kilb, D., Aliyev, A., Gasanov, A., & Yetirmishli, G. (2007). Correlations between
422 earthquakes and large mud volcano eruptions. *Journal of Geophysical Research: Solid*
423 *Earth*, 112(B4).
- 424 Milkov, A. V., Sassen, R., Apanasovich, T. V., & Dadashev, F. G. (2003). Global gas flux from
425 mud volcanoes: a significant source of fossil methane in the atmosphere and the
426 ocean. *Geophysical Research Letters*, 30(2).
- 427 Planke, S., Svensen, H., Hovland, M., Banks, D. A., & Jamtveit, B. (2003). Mud and fluid
428 migration in active mud volcanoes in Azerbaijan. *Geo-Marine Letters*, 23(3-4), 258-268.
- 429 Rao, M. V. M. S., & Lakshmi, K. P. (2005). Analysis of b-value and improved b-value of
430 acoustic emissions accompanying rock fracture. *Current Science*, 1577-1582.
- 431 Rau, R. J., Liang, W. T., Kao, H., & Huang, B. S. (2000). Shear wave anisotropy beneath the
432 Taiwan orogen. *Earth and Planetary Science Letters*, 177(3-4), 177-192.
- 433 Rudolph, M. L., & Manga, M. (2010). Mud volcano response to the 4 April 2010 El Mayor -
434 Cucapah earthquake. *Journal of Geophysical Research: Solid Earth*, 115(B12).
- 435 Rudolph, M. L., & Manga, M. (2012). Frequency dependence of mud volcano response to
436 earthquakes. *Geophysical Research Letters*, 39(14).
- 437 Scholz, C. H. (1968). Experimental study of the fracturing process in brittle rock. *Journal of*
438 *Geophysical Research*, 73(4), 1447-1454.
- 439 Scholz, C. H. (2019). *The mechanics of earthquakes and faulting.* Cambridge university press.
- 440 Shi, Y., & Bolt, B. A. (1982). The standard error of the magnitude-frequency b value. *Bulletin of*
441 *the Seismological Society of America*, 72(5), 1677-1687.
- 442 Snead, R. J., 1964. Active mud volcanoes of Baluchistan, west Pakistan, *The Geographical*
443 *Review*, 54, 545-560.
- 444 Smith, W. D. (1981). The b-value as an earthquake precursor. *Nature*, 289(5794), 136-139.

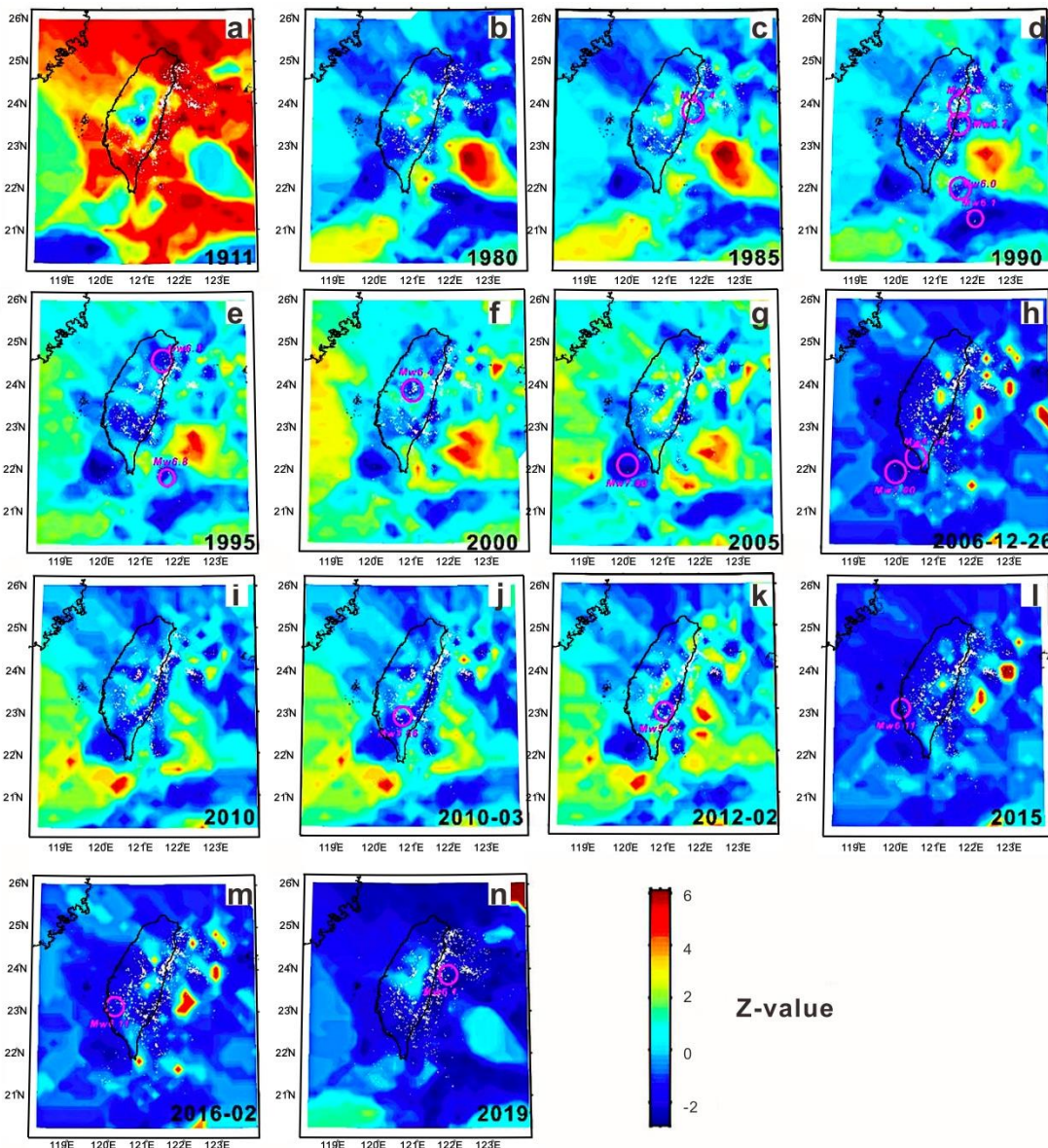
- 445 Sondhi, V. P., 1947. The Makran Earthquake, 28 November 1945, the birth of new islands,
446 Indian Minerals 1, 146–154.
- 447 Sung, Q. C., Chang, H. C., Liu, H. C., & Chen, Y. C. (2010). Mud volcanoes along the Chishan
448 fault in Southwestern Taiwan: A release bend model. *Geomorphology*, 118(1-2), 188-198.
- 449 Wang, C. Y., & Shin, T. C. (1998). Illustrating 100 years of Taiwan seismicity. *Terrestrial,
450 Atmospheric and Oceanic Sciences*, 9(4), 589-614.
- 451 Wang, J. H. (1988). b values of shallow earthquakes in Taiwan. *Bulletin of the Seismological
452 Society of America*, 78(3), 1243-1254.
- 453 Wang, L. Y., Wu, Z. L., & Chen, P. Y. (2004). Correlation between the seismicity
454 parameters. *Acta Seismologica Sinica*, 17(1), 179-185.
- 455 Wiemer, S. (2001). A software package to analyze seismicity: ZMAP. *Seismological Research
456 Letters*, 72(3), 373-382.
- 457 Wiemer, S., & Wyss, M. (1994). Seismic quiescence before the Landers (M= 7.5) and Big Bear
458 (M= 6.5) 1992 earthquakes. *Bulletin of the Seismological Society of America*, 84(3), 900-
459 916.
- 460 Wu, Y. M., & Kanamori, H. (2005). Rapid assessment of damage potential of earthquakes in
461 Taiwan from the beginning of P waves. *Bulletin of the Seismological Society of
462 America*, 95(3), 1181-1185.
- 463 Wu, Y. M., & Zhao, L. (2006). Magnitude estimation using the first three seconds P - wave
464 amplitude in earthquake early warning. *Geophysical Research Letters*, 33(16).
- 465 Wu, Y. M., Chen, C. C., Zhao, L., & Chang, C. H. (2008). Seismicity characteristics before the
466 2003 Chengkung, Taiwan, earthquake. *Tectonophysics*, 457(3-4), 177-182.
- 467 Wyss, M., & Martirosyan, A. H. (1998). Seismic quiescence before the M 7, 1988, Spitak
468 earthquake, Armenia. *Geophysical Journal International*, 134(2), 329-340.
- 469 Wyss, M., Shimazaki, K., & Urabe, T. (1996). Quantitative mapping of a precursory seismic
470 quiescence to the Izu - Oshima 1990 (M6. 5) earthquake, Japan. *Geophysical Journal
471 International*, 127(3), 735-743.
- 472 Yi-Ben, T. (1986). Seismotectonics of Taiwan. *Tectonophysics*, 125(1-3), 17-37.
- 473 Yin, S., Wang, L., Guo, Y., & Zhong, G. (2015). Morphology, sedimentary characteristics, and
474 origin of the Dongsha submarine canyon in the northeastern continental slope of the South
475 China Sea. *Science China Earth Sciences*, 58(6), 971-985.
- 476 You, C. F., Gieskes, J. M., Lee, T., Yui, T. F., & Chen, H. W. (2004). Geochemistry of mud
477 volcano fluids in the Taiwan accretionary prism. *Applied Geochemistry*, 19(5), 695-707.
- 478 Yusifov, M. Z. (2005). Seismic interpretation and classification of mud volcanoes of the South
479 Caspian Basin, offshore Azerbaijan (Doctoral dissertation, Texas A&M University).
- 480



481

482 **Figure 1.** (a) Seismicity zone divisions (A to B) of the Taiwan Island (Wu et al.,2006) and the
 483 mud volcanoes and mud diapirs distribution characteristics in the offshore and onshore SW
 484 Taiwan. Black triangles in the map demarcated the history mud volcanoes (MV) between the
 485 year of 1995 and 2020, while the shadow belt show the directional mud diapirs distributions with
 486 NEE-striking (Chen et al.,2014).The colorful marks show the locations of the historical
 487 earthquakes with the moment magnitude. (b)-(c) The Minimum Magnitude of Completeness
 488 (Mc) and the Goodness of FMD distribution in the SW Taiwan.

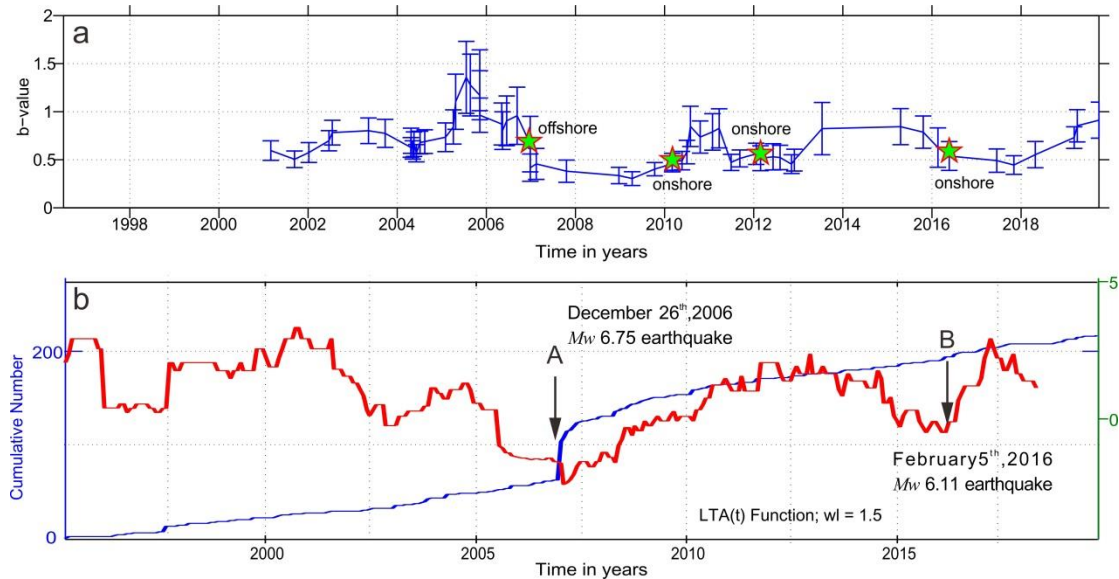
489



490

491 **Figure2** (a)-(n) The seismic rate distribution (z-value) with the time window of 5 years after the
 492 significant earthquakes struck in the vicinity of the Taiwan Island between 1995 and 2020. The
 493 blue area stands for the two or three days before a big earthquake events (The December
 494 26th2006, February 2016 and 2019 Hualian earthquakes) and the z-value show decreasing when

495 approaching a big earthquake. The z-value in the offshore SW Taiwan keep the seismic
 496 quiescence status.



497 **Figure3** (a) b-value changes with time with periodicity fluctuations in the SW Taiwan. Green
 498 stars represent the b-values of the four strong earthquakes in 2006,2010, 2012 and 2016,
 499 respectively. (b) z-value (red line) and the cumulative number (blue line) changes with time in
 501 the SW Taiwan. A and B stand for two abrupt decrease of the z-value subsequent to the two
 502 strong earthquakes.

503

Figure1.

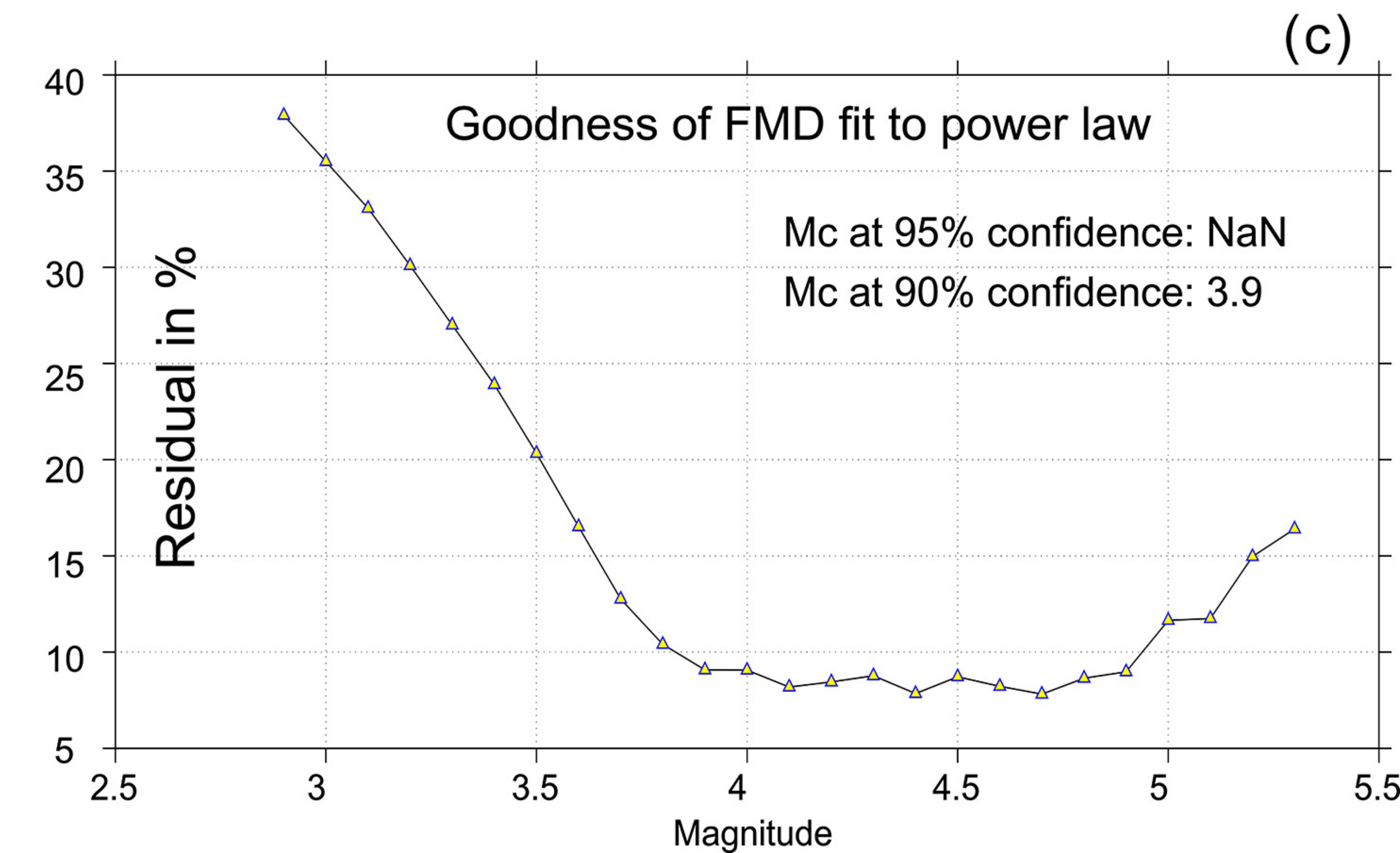
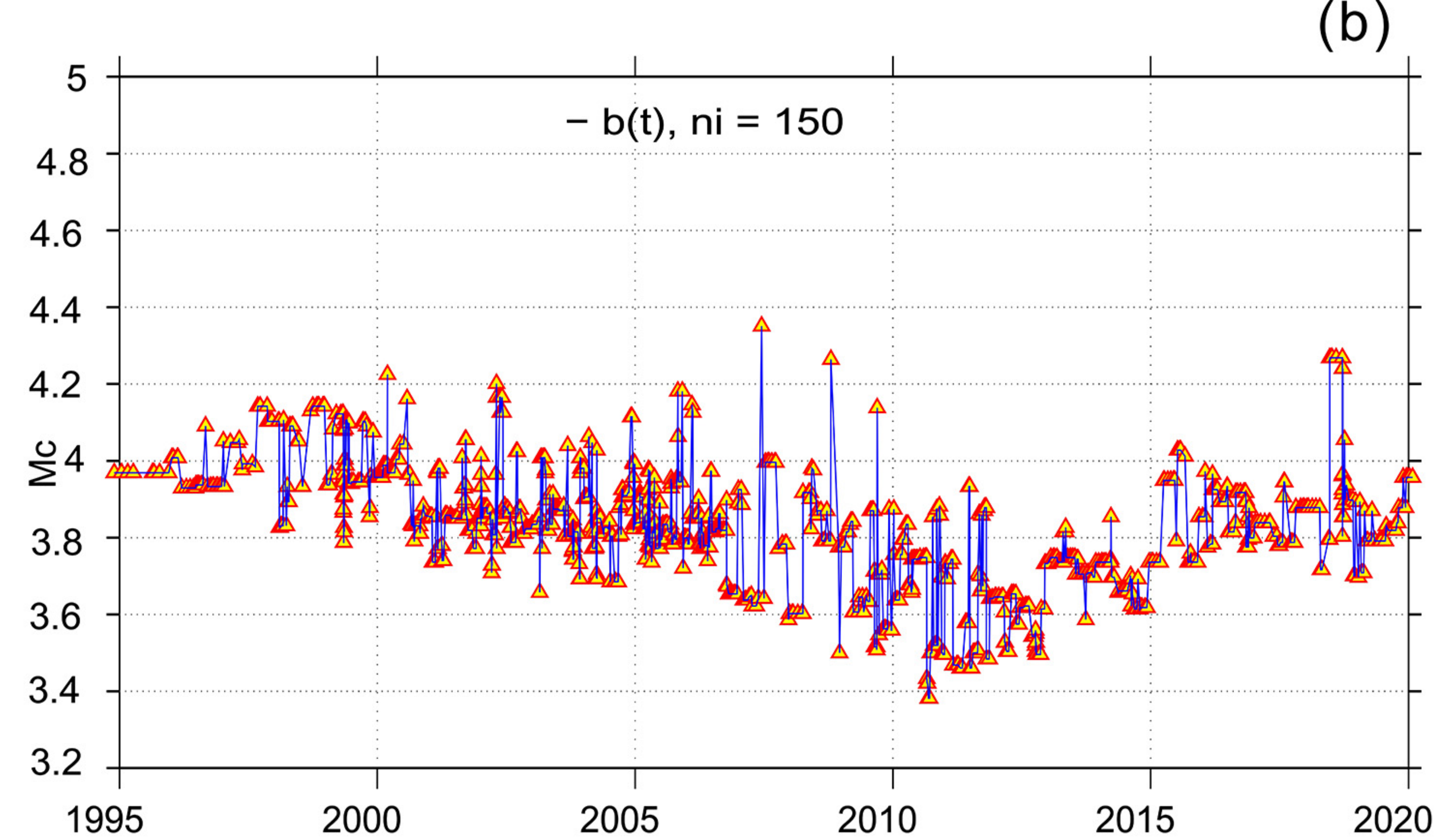
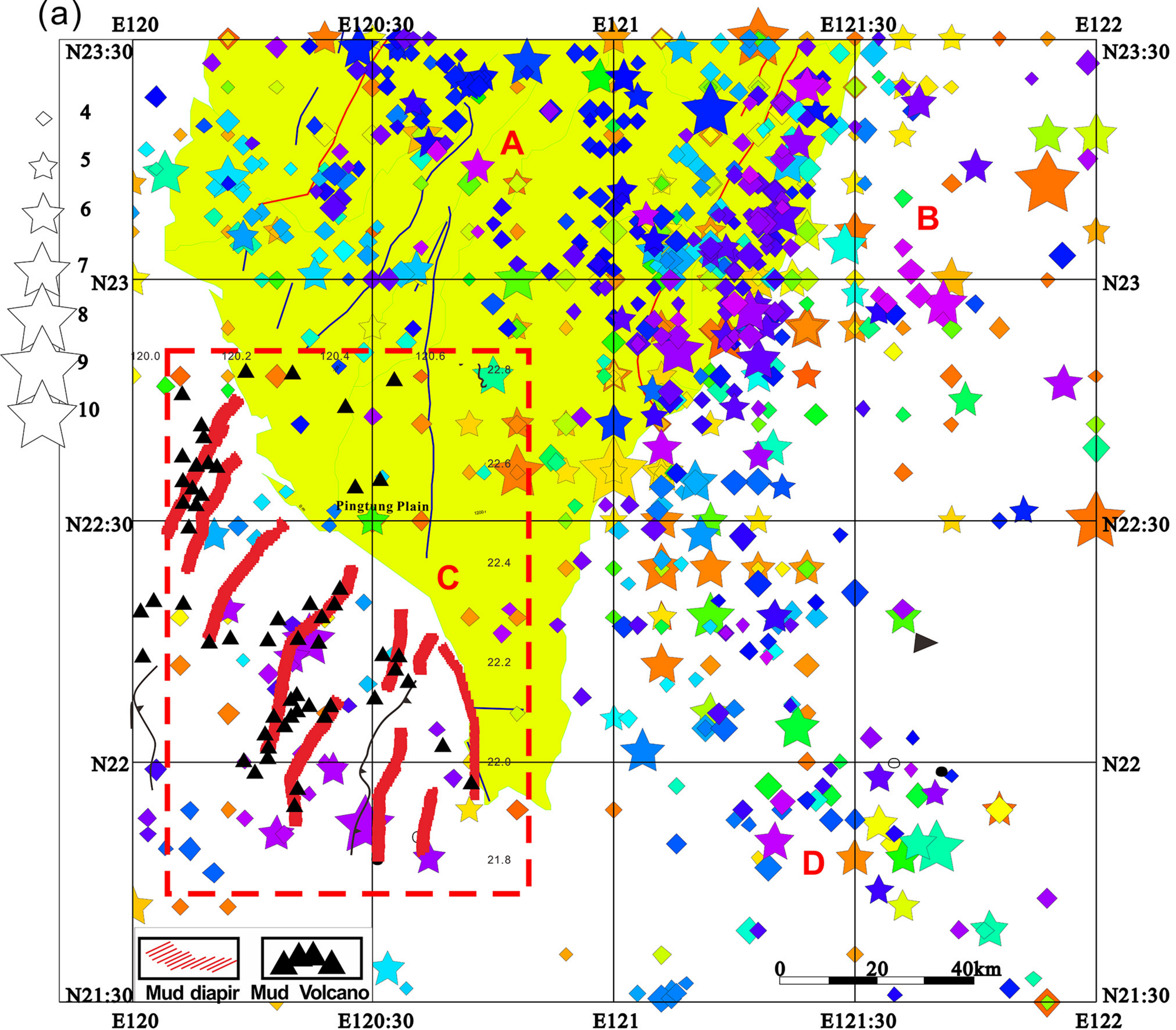


Figure2.

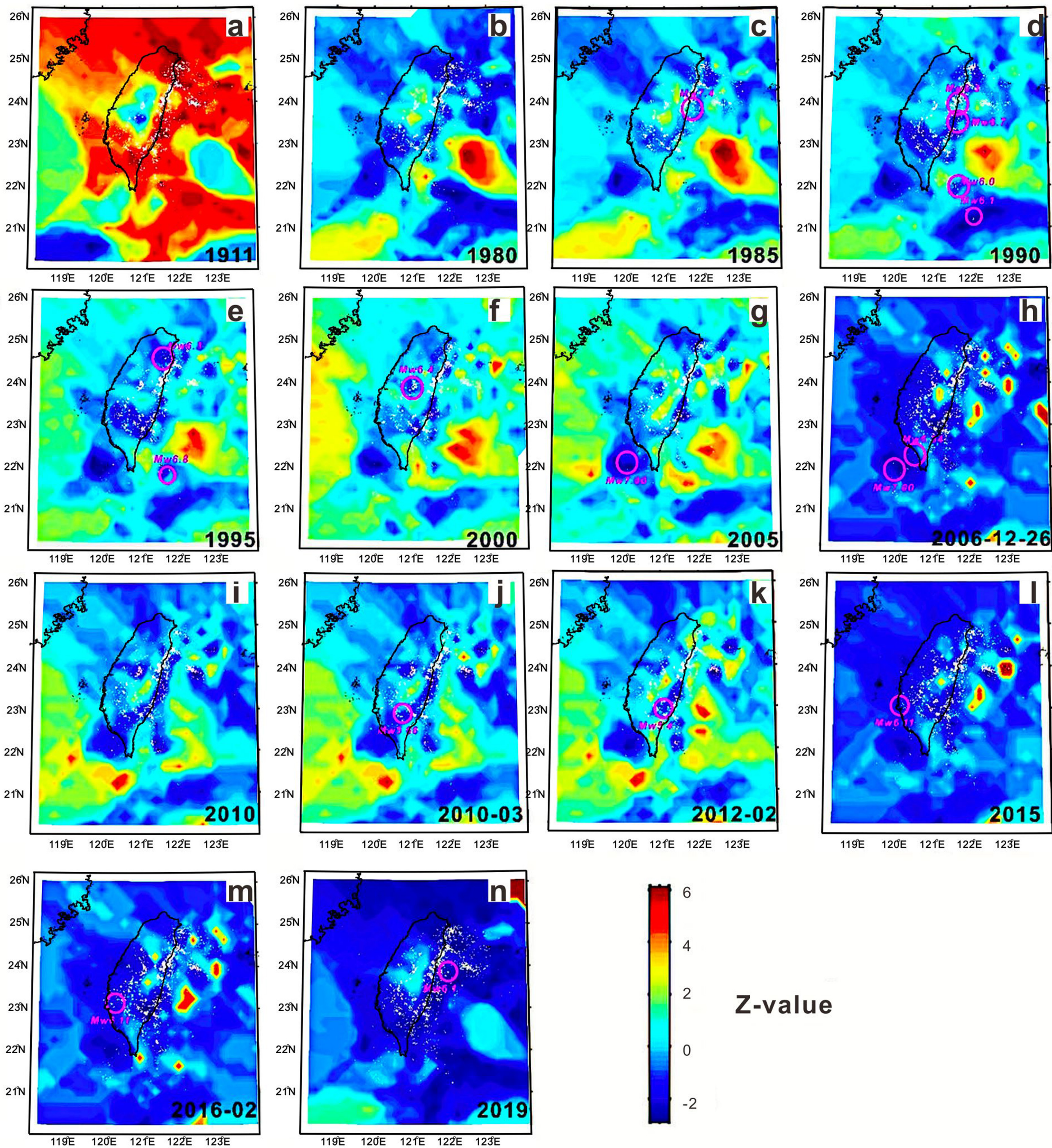


Figure3.

